Cerebral Cortex, April 2021;31: 2026–2037

doi: 10.1093/cercor/bhaa342
Advance Access Publication Date: 7 December 2020
Original Article

ORIGINAL ARTICLE

Postnatal Development of Glutamate and GABA Transcript Expression in Monkey Visual, Parietal, and Prefrontal Cortices

Gil D. Hoftman[1], H. Holly Bazmi[2], Andrew J. Ciesielski[2], Liban A. Dinka[2], Kehui Chen[3] and David A. Lewis[2]

[1]Department of Psychiatry, University of California, Los Angeles, CA 90095, USA, [2]Department of Psychiatry, School of Medicine, University of Pittsburgh, Pittsburgh, PA 15213, USA and [3]Department of Statistics, School of Arts and Sciences, University of Pittsburgh, Pittsburgh, PA 15213, USA

Address correspondence to David A. Lewis, Department of Psychiatry, University of Pittsburgh, BST W1653, 3811 O'Hara Street, Pittsburgh, PA 15213, USA. Email: lewisda@upmc.edu.

Abstract

Visuospatial working memory (vsWM) requires information transfer among multiple cortical regions, from primary visual (V1) to prefrontal (PFC) cortices. This information is conveyed via layer 3 glutamatergic neurons whose activity is regulated by gamma-aminobutyric acid (GABA)ergic interneurons. In layer 3 of adult human neocortex, molecular markers of glutamate neurotransmission were lowest in V1 and highest in PFC, whereas GABA markers had the reverse pattern. Here, we asked if these opposite V1–visual association cortex (V2)–posterior parietal cortex (PPC)–PFC gradients across the vsWM network are present in layer 3 of monkey neocortex, when they are established during postnatal development, and if they are specific to this layer. We quantified transcript levels of glutamate and GABA markers in layers 3 and 6 of four vsWM cortical regions in a postnatal developmental series of 30 macaque monkeys. In adult monkeys, glutamate transcript levels in layer 3 increased across V1–V2–PPC–PFC regions, whereas GABA transcripts showed the opposite V1–V2–PPC–PFC gradient. Glutamate transcripts established adult-like expression patterns earlier during postnatal development than GABA transcripts. These V1–V2–PPC–PFC gradients and developmental patterns were less evident in layer 6. These findings demonstrate that expression of glutamate and GABA transcripts differs across cortical regions and layers during postnatal development, revealing potential molecular substrates for vsWM functional maturation.

Key words: cortical regions, development, GABA, glutamate, working memory

Introduction

Visuospatial working memory (vsWM), the ability to maintain and manipulate a limited amount of visuospatial information to guide goal-directed thought and behavior (Baddeley 1992; Barch and Ceaser 2012), is mediated in primates, at least in part, by a widely distributed cortical network that links multiple regions in the occipital (e.g., primary visual [V1] and visual association [V2]), posterior parietal (PPC), and dorsolateral prefrontal (PFC) cortices (Miller and Cohen 2001; Linden 2007; Arnsten 2015). In this network, layer 3 glutamatergic pyramidal neurons convey feedforward vsWM information from the occipital regions to the PPC and PFC and feedback information from the PFC to the PPC (Felleman and Van Essen 1991; Rockland 1997). Within each cortical region, gamma-aminobutyric acid (GABA)ergic interneurons regulate the activity of layer 3 pyramidal neurons, contributing to the synchronization of neuronal firing associated with vsWM (Goldman-Rakic 1995; Wang et al. 2004).

In human neocortex, we recently reported that indices of glutamate and GABA neurotransmission in layer 3 showed opposite V1–V2–PPC–PFC gradients across regions of the vsWM

network, with glutamate markers lower in V1 and higher in PFC, whereas GABA markers were higher in V1 and lower in PFC (Hoftman et al. 2018). In subjects with schizophrenia, an illness characterized by impairments in vsWM, these glutamate and GABA transcript gradients were differentially altered; relative to unaffected comparison subjects, subjects with schizophrenia had a blunted glutamate gradient, with transcript levels higher in V1 and lower in PFC, and an enhanced GABA gradient, with transcript levels higher in V1 and lower in PFC (Hoftman et al. 2018). However, understanding the potential mechanism(s) and functional consequences of these disease-associated shifts in markers of glutamate and GABA neurotransmission requires studies that can only be conducted in a model system. Thus, to facilitate such investigations, the goals of the present studies were 3-fold.

First, we sought to determine if the opposite V1–V2–PPC–PFC gradients in glutamate and GABA transcript levels normally present in layer 3 across the human cortical vsWM network are also present across the homologous regions of the macaque monkey neocortex. Because the monkey and human vsWM networks share many features and some markers of glutamate- and GABA-related transcripts appear to have high (or low) levels in V1 and low (or high) levels in PFC in total gray matter from monkeys and humans (Kang et al. 2011; Hawrylycz et al. 2012; Jaffe et al. 2018), we predicted that mature monkeys would exhibit the same opposite glutamate and GABA cortical gradients observed in layer 3 of adult humans.

Second, we sought to characterize the postnatal developmental trajectories of cortical glutamate and GABA transcripts in layer 3 of the monkey vsWM network. Such studies are necessary to gain insight into the possible neural substrate for schizophrenia-associated working memory impairments which frequently arise during childhood and progress before the onset of psychosis during late adolescence or early adulthood (Reichenberg et al. 2010; Niendam et al. 2018). Some indices of cortical maturation are achieved earlier in caudal sensory cortices than in rostral association cortices (Condé et al. 1996; Sowell et al. 2003; Tamnes et al. 2010), whereas synaptogenesis has been reported to be synchronous across the monkey neocortex (Rakic et al. 1986). Since glutamate and GABA neurotransmission is important for postnatal synapse maturation and stability (Lardi-Studler and Fritschy 2007), we predicted that glutamate and GABA transcripts would reach mature levels synchronously across the cortical vsWM network prior to the adult period.

Third, we sought to determine if the presence and developmental trajectories of the glutamate and GABA gradients across the vsWM network differ between layers 3 and 6. This comparison is of interest because both excitatory and inhibitory neurons appear to be altered in layer 3, but not in layer 6, in the PFC of subjects with schizophrenia (Akbarian et al. 1995; Rajkowska et al. 1998; Volk et al. 2000; Kolluri et al. 2005). These two layers also provide interesting contrasts because their excitatory neurons have different projection targets (i.e., primarily cortical for layer 3 vs. thalamic for layer 6) and they are differentially enriched for subtypes of GABA neurons (Jones 1984; Condé et al. 1994). In addition, the peripubertal period coincides with the excitatory synaptic pruning in the PFC that appears to be more pronounced in layer 3 than in layer 6 (Bourgeois et al. 1994; Huttenlocher and Dabholkar 1997; Petanjek et al. 2011). Given that cortical laminar development proceeds in an inside-out pattern such that deeper layers are established prior to superficial layers (Rakic 1974, 2009), we predicted that the developmental gradients for glutamate and GABA measures would be more protracted in layer 3 than in layer 6.

To test these predictions, we quantified transcript levels of the same markers of glutamate and GABA neurotransmission that we previously studied in the human vsWM cortical network in both layers 3 and 6 of the four homologous cortical regions from a developmental series of macaque monkeys.

Materials and Methods

Animals and Tissue Preparation

Rhesus (*Macaca mulatta*) monkeys ($n = 30$) ranging in age from postnatal 3 days to 12 years (middle adulthood) old were used in this study (Table 1). Tissue samples were obtained from an existing bank of monkey brain tissue assembled from prior studies (Gonzalez-Burgos et al. 2008; Datta et al. 2015; Chung et al. 2017; Dienel et al. 2017). Only tissue samples from female animals were available for use in this study because the male animals from this breeding program were all committed to invasive studies conducted by another research group. As previously reported, monkeys younger than 6 months of age were housed with their mothers, juveniles 6–24 months of age were housed in groups, and those older than 24 months of age were housed either in pairs or in single cages in the same social setting. All animals had been euthanized as part of prior studies: five animals were perfused transcardially with ice-cold artificial cerebrospinal fluid under deep anesthesia with ketamine and pentobarbital, and the remaining 25 monkeys were deeply anesthetized with ketamine and pentobarbital without transcardial perfusion (Gonzalez-Burgos et al. 2008; Datta et al. 2015; Chung et al. 2017; Dienel et al. 2017). For all animals, the brain was removed intact and the right hemisphere was blocked, flash-frozen in isopentane, and stored at −80 °C as previously described (Dienel et al. 2017). All housing and experimental procedures were conducted in accordance with the guidelines of the US Department of Agriculture and the National Institutes of Health Guide for the Care and Use of Laboratory Animals and with the approval of the University of Pittsburgh Institutional Animal Care and Use Committee.

Laser Microdissection Procedure

Four neocortical regions [V1, V2, PPC (area 7), PFC (areas 9/46)] were identified based on their anatomical locations and characteristic cytoarchitectonic features (Walker 1940; Lund et al. 1977; Pandya and Seltzer 1982; Lewis and Van Essen 2000) (Fig. 1A,B). For each region, cryostat sections (12 µm) were cut, thaw-mounted onto glass polyethylene naphthalate membrane slides (LEICA Microsystems) which were coded to blind subject number and age, dried, and stored at −80 °C as previously described (Datta et al. 2015). On the day of microdissection, tissue sections were stained for Nissl substance with thionin, and the borders of cortical layers were identified based on their distinctive cytoarchitecture (Fig. 1C). The clear borders between layers 2–3 and 3–4 were used to capture the layer 3 samples. Because the border between layers 5 and 6 is less sharply delineated, the layer 6 sampling procedure was operationalized by (1) identifying the distinct borders between layers 4 and 5 and between layer 6 and the white matter (WM), (2) determining the midpoint between these two borders, and (3) collecting the cortical tissue between the midpoint and the layer 6 WM. To ensure comparable sampling of both layers across regions, a

Table 1. Monkey developmental cohort

Age group[a]	Monkey	Age (months)	Sex	Weight (kg)	Perfusion status	Storage time (months)
Postnatal	315	0.1	M	0.7	–	214
	311	0.23	F	0.7	–	97
	194	0.23	F	N/A	–	237
	199	0.23	F	0.5	–	225
	201	0.23	F	0.4	–	224
	331	0.27	F	0.6	–	47
	299	1	F	0.6	–	123
	319	1	F	0.7	+	84
	306	1.5	F	0.7	+	110
Prepubertal	277	3	F	1.0	+	149
	310	3	F	1.1	–	98
	324	3	F	1.1	–	72
	294	8	F	1.8	–	128
	261	9	F	1.6	–	160
	262	9	F	1.8	–	160
	317	16	F	2.7	–	214
	287	18	F	2.4	–	132
	286	19	F	2.4	–	132
Peripubertal	297	30	F	4.9	–	124
	298	30	F	4.2	–	124
	291	32	F	3.9	–	130
	289	45	F	5.7	–	132
	258	46	F	6.3	+	161
	288	47	F	5.0	–	132
Adult	335	60	F	7.0	–	45
	340	60	F	8.1	–	44
	343	60	F	6.0	–	44
	326	96	F	14.0	–	72
	259	104	F	6.4	+	160
	354	144	F	7.7	–	38

Note: [a]Postnatal, rising phase of excitatory synapse density, 0.1–1.5 months; prepubertal, plateau phase with stable levels of excitatory synapses prior to puberty onset, 3–19 months; peripubertal, declining phase of excitatory synapses (pruning) during puberty, 30–47 months; and adult, mature phase with stable adult levels of excitatory synapses, 60–144 months.

LEICA microdissection system (LMD 6500; 5x objective) was used to collect samples containing the same tissue volume from portions of each section which were cut perpendicular to the pial surface. Each sample (composed of a cross-sectional area of approximately 5 million μm^2 x 12 µm thick sections) contained ~60 million μm^3 of tissue which yielded sufficient high-quality RNA for reliable quantification of 12 transcripts.

Quantitative Polymerase Chain Reaction

For each sample, total RNA was converted to complementary DNA using the SuperScript IV VILO Master Mix (Thermo Fisher Scientific). Forward and reverse primers were designed to target transcripts whose cognate proteins are known to regulate the key components of glutamate and GABA neurotransmission. To compare results with findings from our prior study of layer 3 in the human vsWM network (Hoftman et al. 2018), we quantified levels of the same five glutamate and four GABA transcripts. These transcripts include the following functionally analogous markers of glutamate and GABA neurotransmission: (1) the enzymes that synthesize most cortical glutamate and GABA, glutaminase (GLS1) and the 67 kD isoform of glutamic acid decarboxylase (GAD67), respectively; (2) the cortical vesicular glutamate (vGLUT1) and GABA (vGAT) transporters that package their respective neurotransmitters into presynaptic vesicles; (3) the excitatory amino acid (EAAT2) and GABA (GAT1) membrane transporters involved in perisynaptic glutamate and GABA neurotransmitter reuptake, respectively; and (4) the obligatory N-methyl-D-aspartate (NMDA) receptor NR1 subunit (GRIN1), the calcium-impermeable AMPA receptor GluR2 subunit (GRIA2), and the obligatory ionotropic GABA ($GABA_A$) receptor subunit $\gamma 2$ (GABRG2). For EAAT2, the target transcript was EAAT2A isoform/variant 1, and for GRIA2, the target transcript was the synapse-enriched flip isoform (variants 1 and 3). Our experimental design, which controlled for batch effects across regions and layers within subjects (i.e., each 384 well qPCR plate included quadruplicate measures of nine target and three housekeeping transcripts for four regions and two layers from each subject) necessarily limited the number of transcripts that could be studied and thus excluded the possibility of examining other glutamate or GABA receptor transcripts or other isoforms of the targeted transcripts.

All primers showed 90–100% efficiency, and each amplified product resulted in a single and specific amplicon (see Supplementary Table S1). Three housekeeping genes (β-actin [AB], cyclophilin-A [Cyclo], and the guanine nucleotide-binding protein alpha subunit [GNAS]), selected based on their stable expression in prior monkey developmental studies (Datta et al. 2015; Hoftman et al. 2015; Dienel et al. 2017), were used to normalize the target transcript expression levels.

Each transcript was quantified by qPCR using Power SYBR Green fluorescence and the ViiA™7 Real Time PCR System. Cycle

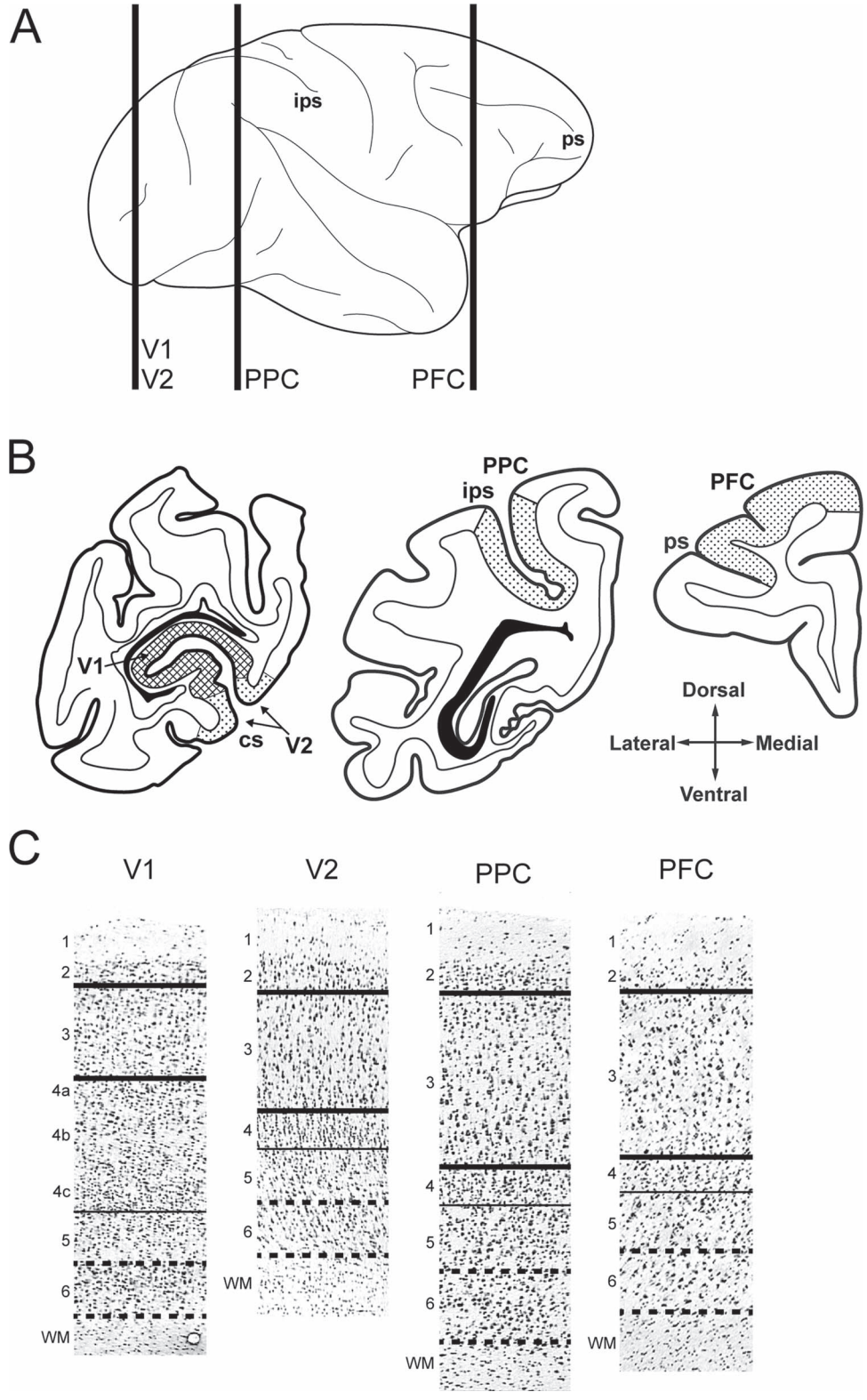

Figure 1. Sampling of cortical regions and layers in rhesus macaque monkeys. (*A*) Lateral view of rhesus macaque neocortex. Vertical lines indicate the approximate location of the three tissue blocks sampled for this study. (*B*) Coronal view of tissue blocks containing the regions studied including V1, V2, PPC, and PFC. Hatched areas indicate approximate locations where layers 3 and 6 samples were captured by laser microdissection. Compass indicates tissue orientation. (*C*) Nissl-stained tissue sections before laser microdissection showing representative cytoarchitecture in each cortical region studied. Numbers indicate cortical layers. The pia was removed from each panel. Thick solid lines indicate microdissection boundaries for layer 3 samples, thin solid lines indicate the layer 4–5 border, and thick dashed lines indicate the microdissection boundaries for layer 6 samples. cs, calcarine sulcus; ips, intraparietal sulcus; ps, principal sulcus.

threshold (CT) values were assessed for the normalizers and each gene of interest in quadruplicate, and the delta CT (dCT) for each target transcript was calculated by subtracting the mean CT of the three normalizer genes from the CT of the gene of interest. Because the dCT represents the log2-transformed expression ratio of each target transcript to the mean of the normalizer genes, the relative expression levels of the target transcripts are reported as the more intuitive expression ratio, or the 2^{-dCT}.

Statistical Analysis

To visualize the general effect of age on transcript levels, we plotted data from each animal on a log scale for age and on a linear scale for transcript level (see Supplementary Figs S1 and S2). A semi-log linear fit was computed for each transcript in layers 3 and 6; examination of other linear and nonparametric approaches suggested overfitting of the data, although there was a moderate nonlinear trend in some of the plots. For all transcripts studied, and within each age group, the perfusion status had no apparent effect on transcript levels similar to an absence of effect of the perfusion status reported in previous studies (Datta et al. 2015; Hoftman et al. 2015; Dienel et al. 2017).

For statistical assessments, each animal was assigned to one of four age groups. These age groups were defined by the developmental trajectory of excitatory synapse and dendritic spine densities in layer 3 of monkey neocortex. Given that the largest body of literature on the developmental time course of these measures is in the monkey PFC (Rakic et al. 1986; Bourgeois and Rakic 1993; Bourgeois et al. 1994; Anderson et al. 1995), those data were used to define the following age groups: postnatal, the period after birth when the excitatory synaptic density is increasing; prepubertal, the period when the excitatory synapse density is at a stable plateau; peripubertal, the period of the excitatory synaptic pruning; and adult, the period when the density of the excitatory synapses is at stable mature levels. For this study, the ages included in each group are as follows: postnatal, 0.1–1.5 months; prepubertal, 3–19 months; peripubertal, 30–47 months, and adult, 60–144 months.

To compare transcript levels across regions, a mixed-model for each layer treating observations from the four regions for each monkey as repeated measures was performed for each transcript and for each composite measure. Composite scores of the glutamate and GABA measures were computed by summing the normalized (Z-score) expression levels for all glutamate and GABA transcripts, respectively, as previously described (Hoftman et al. 2018; Dienel et al. 2019). Each model included transcript as the dependent variable; region, age group, and their interactions as fixed effects; monkey as random effect; and qPCR batch and tissue storage time as covariates. Batch and tissue storage time did not have a significant effect on the levels of any transcript across age groups or regions. In the final model, *F*-tests were used to assess the overall region, age group, and age group-specific regional effects, as well as the region-by-age group interaction effects, followed by post hoc pairwise comparisons between regions and age groups.

To compare transcript levels across regions and layers, a mixed-model treating observations from the four regions and two layers for each monkey as repeated measures was performed for each transcript and for each composite measure. The model included transcript as the dependent variable; region, layer, age group, and their interactions as fixed effects; subject and layer (nested in subject, which accounts for the hierarchical correlation structures within each subject and layer) as random effect; and qPCR batch and tissue storage time as covariates. Batch and tissue storage time did not have a significant effect on the levels of any transcript across age groups, regions, or layers. *F*-tests were first used to assess the interaction effects. Because neither layer-by-age or layer-by-age-by-region interaction effects were significant for any transcripts, these two interactions were omitted from the final model. In the final model, *F*-tests were used to assess the overall region, age group and layer effects, the layer-specific and age group-specific regional effects, and the region-by-layer and region-by-age interaction effects, followed by post hoc pairwise comparisons between regions, layers, and age groups.

All analyses were conducted on log-transformed data to stabilize the variance. For all analyses, the uncorrected *P*-values are reported in the main text, with $P < 0.005$ set as the Bonferroni corrected significance threshold. Models used SAS version 9.3 (SAS Institute) to implement PROC MIXED using the restricted maximum likelihood method with the default ("containment") method used to compute the denominator degrees of freedom (DOF). In our study design, for each transcript, we have total 240 observations (30 subjects × 2 layers × 4 regions). Using the containment method, the DOF for between subject factors (e.g., age) is computed to be 24 (which basically only counts independent factors), and the DOF for within subject factors (e.g., region and layer) is adjusted to be 164.

Results

Cortical Glutamate and GABA Transcript Gradients in Layer 3 of the Adult Monkey vsWM Network

In layer 3 of the adult monkeys, the effect of cortical region was highly significant for many of the glutamate and GABA transcripts studied (Fig. 2). For glutamate transcripts (Fig. 2, left column), the effect of region was significant (all $F_{3,78} > 9.5$; $P < 0.00002$) for GLS1, vGLUT1, and GRIA2 levels, but not for EAAT2 and GRIN1 levels (both $F_{3,78} < 0.5$; $P > 0.72$). For GABA transcripts (Fig. 2, right column), the effect of region was significant (all $F_{3,78} > 7.3$; $P < 0.00003$) for vGAT, GAT1, and GABRG2 levels, but not for GAD67 ($F_{3,78} = 1.6$; $P = 0.20$). For all transcripts, the effect of region, when present, was principally due to the differences between V1 and PFC, with V2 and PPC mostly having intermediate values.

Consistent with the most common patterns for the individual transcripts in layer 3, the composite measure of all five glutamate transcripts in the adult monkeys showed a V1–V2–PPC–PFC gradient of low-to-high ($F_{3,78} = 8.4$; $P = 0.00007$) (Fig. 3G), whereas the composite measure of all four GABA transcripts showed the opposite high-to-low gradient from V1–V2–PPC–PFC ($F_{3,78} = 7.2$; $P = 0.0002$) (Fig. 3H). Both gradients were qualitatively similar to those we previously observed in layer 3 across the homologous regions of the adult human vsWM cortical network (Hoftman et al. 2018).

Emergence and Maturation of Glutamate and GABA Composite Transcript Gradients in Layer 3

To determine when the regional patterns of glutamate and GABA composite transcript levels in layer 3 emerged during postnatal development, we calculated the region-by-age group interaction effect. For the glutamate composite measure, the overall region-by-age group interaction effect was significant

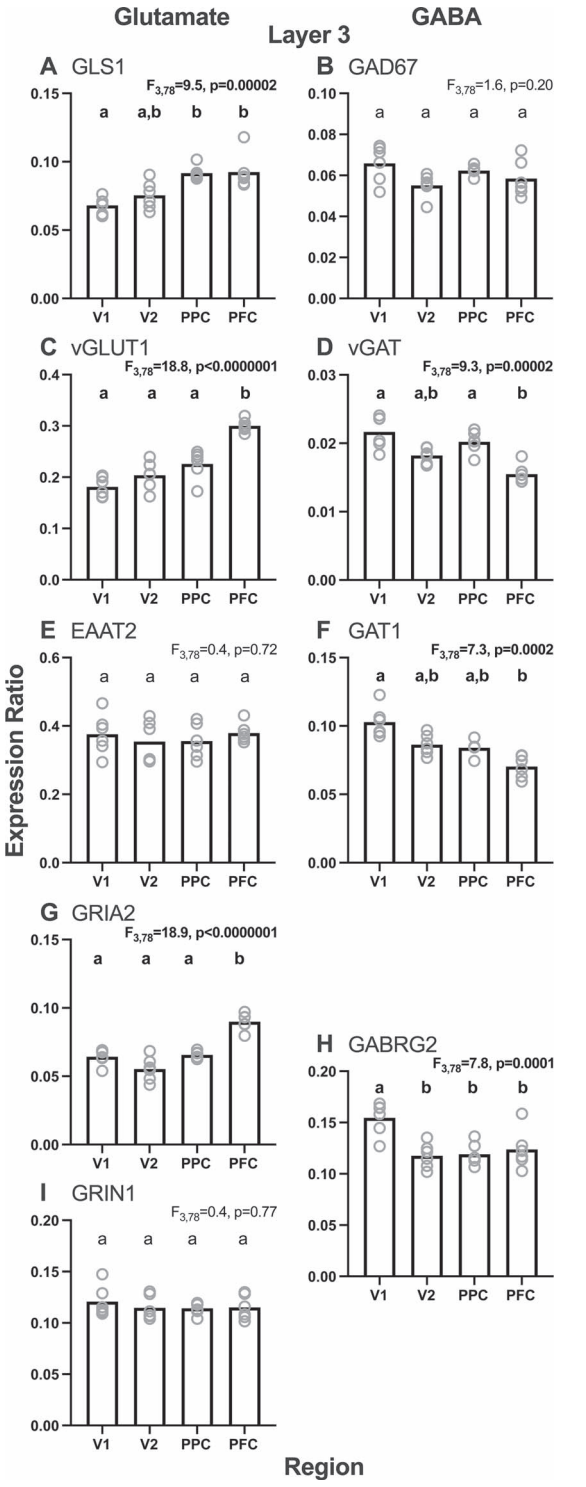

Figure 2. Layer 3 regional gradients for each glutamate (left column) and GABA (right column) transcript studied from the adult monkey age group (adult, 60–144 months). Bars represent group means and circles represent individual subject data. Within each graph, bars not sharing the same lower-case letter are significantly different. GLS1 = glutaminase; vGLUT1 = vesicular glutamate transporter 1; EAAT2 = excitatory amino acid transporter 2; GRIA2 = AMPA receptor GluR2 subunit; GRIN1 = NMDA receptor NR1 subunit; GAD67 = glutamic acid decarboxylase, 67 kD isoform; vGAT = vesicular GABA transporter; GAT1 = GABA transporter 1; GABRG2 = GABAA receptor $\gamma 2$ subunit.

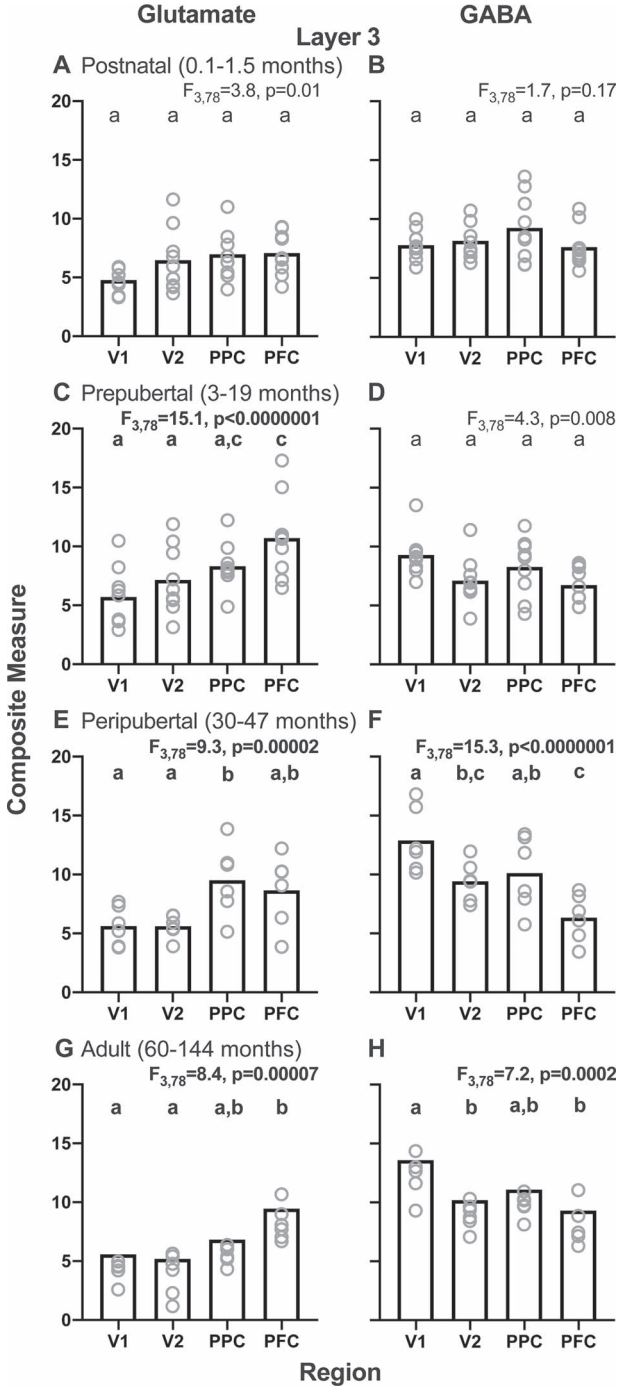

Figure 3. Layer 3 glutamate and GABA composite measures for each of four postnatal age groups (postnatal, 0.1–1.5 months; prepubertal, 3–19 months; peripubertal, 30–47 months; and adult, 60–144 months) across regions of the cortical vsWM network in monkeys. Left column shows glutamate composite measures and right column shows GABA composite measures for each age group. Note the opposite V1–V2–PPC–PFC gradients for the glutamate composite measure in the prepubertal, peripubertal, and adult age groups and for the GABA composite measure in the peripubertal and adult age groups. Bars represent group means, and circles represent individual subject data. Within each graph, bars not sharing the same lower-case letter are significantly different.

($F_{9,78} = 2.6$; $P = 0.01$). These regional differences, with PFC > V1, first appeared in the prepubertal period (Fig. 3C). For the GABA composite measure, the overall region-by-age group interaction effect was significant ($F_{9,78} = 3.7$; $P = 0.0007$). These regional differences, with V1 > PFC, first appeared in the peripubertal period (Fig. 3F). These findings suggest that the glutamate composite regional differences arise earlier during the postnatal development than do the GABA composite regional differences.

Cortical Glutamate and GABA Transcript Gradients are Less Pronounced in Layer 6

In layer 6 of the adult monkeys (Fig. 4), the effect of region was significant for EAAT2 and GRIA2 transcript levels ($F_{3,77} > 6.3$; $P < 0.0007$), but not for GLS1, vGLUT1, or GRIN1 ($F_{3,77} < 3.6$; $P > 0.02$). The effect of region, when present, was due principally to lower transcript levels in V1 and V2 relative to PPC and PFC (Fig. 4, left column). For GABA transcripts, the effect of region was significant for GABRG2 levels ($F_{3,77} = 21.8$; $P < 0.0000001$), but not significant (all $F_{3,77} < 1.2$; $P > 0.32$) for GAD67, vGAT, GAT1 levels (Fig. 4, right column). The effect of region for GABRG2 was due to higher levels in V1 compared with V2, PPC, and PFC.

Consistent with most individual transcripts in the adult animals, the effect of region was not significant on the glutamate composite measure ($F_{3,77} = 1.9$; $P = 0.14$) (Fig. 5G) or the GABA composite measure ($F_{3,77} = 2.3$; $P = 0.06$) (Fig. 5H). Across age groups, the glutamate composite measure did differ significantly by region in the pre- and peripubertal periods ($F_{3,77} > 6.1$; $P < 0.0009$) (Fig. 5, left column). However, the GABA composite measure did not differ by region in any of the four postnatal age groups ($F_{3,77} < 2.5$; $P > 0.06$) (Fig. 5, right column).

The more prominent regional gradients in layer 3 relative to layer 6 might reflect, at least in part, the higher levels of both the glutamate and GABA composite measures in layer 3 than in layer 6 across regions for each age group (compare corresponding panels of Figs 3 and 5).

Discussion

In this study, we found that transcript markers of glutamate and GABA neurotransmission in layer 3 exhibited opposite regional gradients in the adult monkey vsWM network, with glutamate transcript levels increasing and GABA transcript levels decreasing from V1–V2–PPC–PFC. These regional differences were first evident earlier in the development for the glutamate composite measure (prepubertal, 3- to 19-month-old animals) than for the GABA composite measure (peripubertal, 30- to 47-month-old animals). Finally, the regional gradients were more pronounced in layer 3 than in layer 6 for both glutamate and GABA transcripts.

Consistent with our first prediction, glutamate and GABA transcript levels had opposite V1–V2–PPC–PFC gradients in layer 3 of adult monkeys similar to those previously reported in adult humans (Hoftman et al. 2018). These regional differences in the glutamate composite measure might be related to variations in the structural properties of layer 3 pyramidal neurons across the monkey cortical vsWM network. For example, both the size of layer 3 pyramidal neuron dendritic arbors and the density of dendritic spines increase from V1 to PPC to PFC (Elston et al. 2001; Elston 2003; Chaudhuri et al. 2015; Medalla and Luebke 2015; Gonzalez-Burgos et al. 2019). The resulting marked regional differences in the total number of layer 3 dendritic

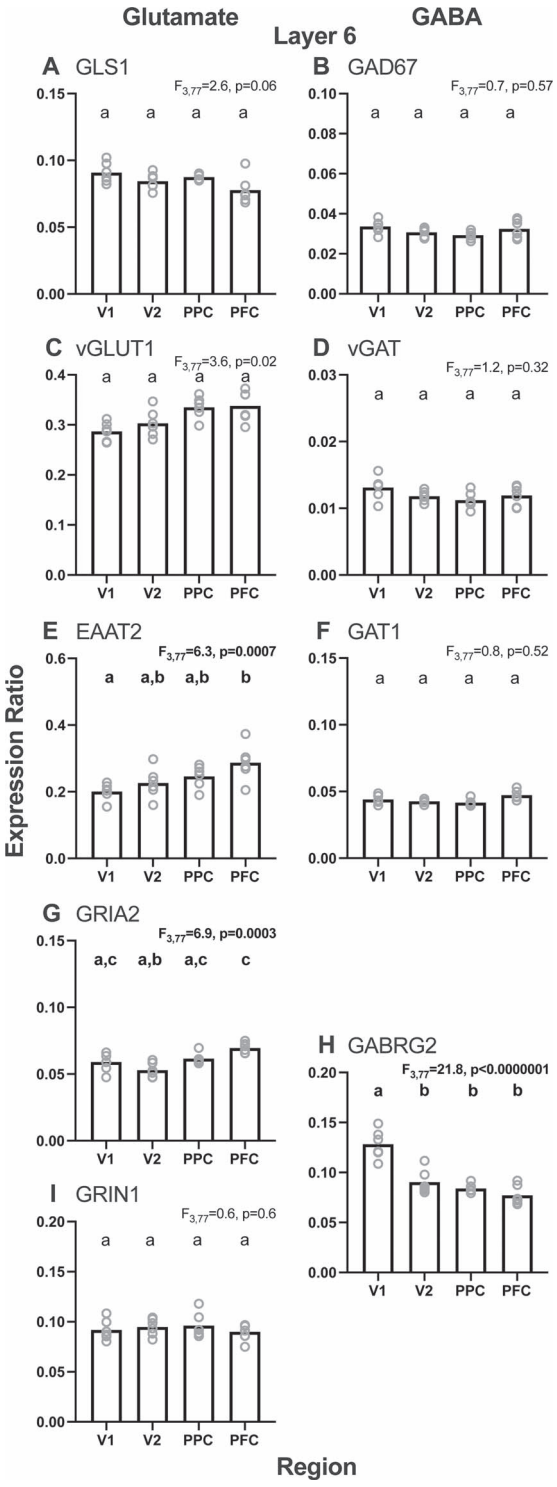

Figure 4. Layer 6 regional gradients for each glutamate (left column) and GABA (right column) transcript studied from the adult monkey age group (adult, 60–144 months). Bars represent group means and circles represent individual subject data. Within each graph, bars not sharing the same lower-case letter are significantly different. GLS1 = glutaminase; vGLUT1 = vesicular glutamate transporter 1; EAAT2 = excitatory amino acid transporter 2; GRIA2 = AMPA receptor GluR2 subunit; GRIN1 = NMDA receptor NR1 subunit; GAD67 = glutamic acid decarboxylase, 67 kD isoform; vGAT = vesicular GABA transporter; GAT1 = GABA transporter 1; GABRG2 = GABAA receptor $\gamma 2$ subunit.

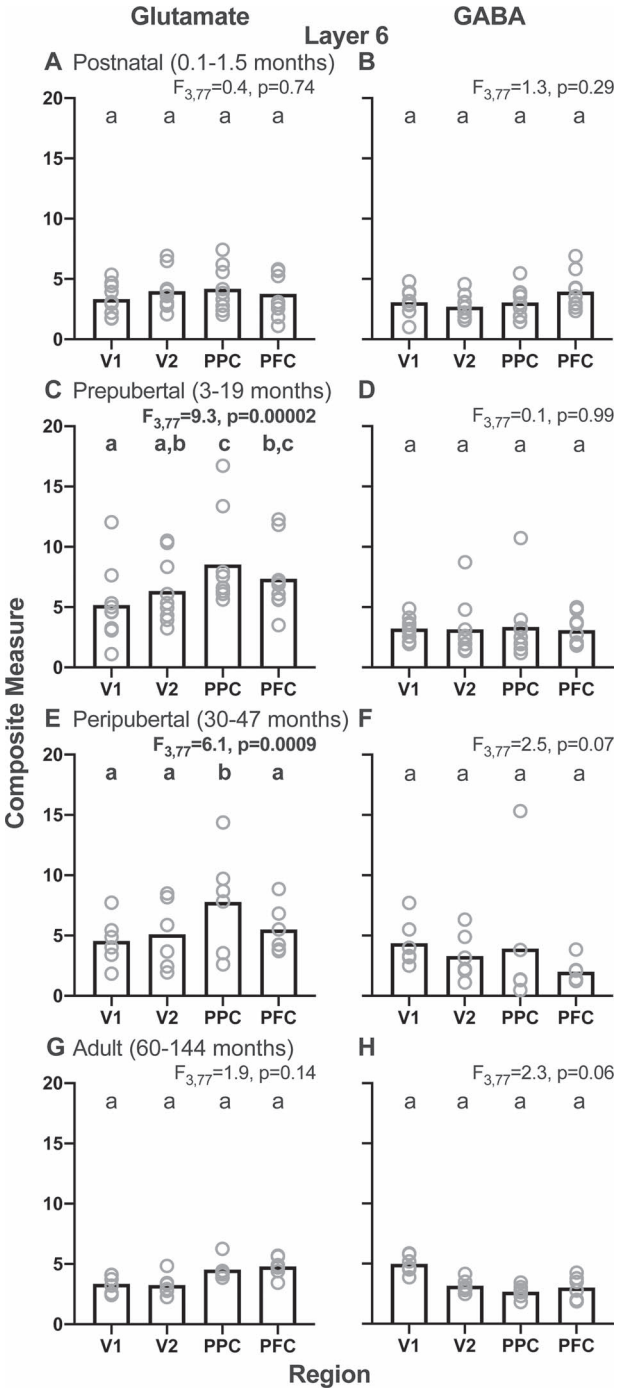

Figure 5. Layer 6 glutamate and GABA composite measures for each of four postnatal age groups (postnatal, 0.1–1.5 months; prepubertal, 3–19 months; peripubertal, 30–47 months; and adult, 60–144 months) across regions of the cortical vsWM network in monkeys. Left column shows glutamate composite measures and right column shows GABA composite measures. Bars represent group means and circles represent the individual subject data. Within each graph, bars not sharing the same lower-case letter are significantly different.

spines, each of which receives an excitatory synapse, would likely be reflected in comparable regional differences in markers of glutamate neurotransmission as found in the present study. In contrast, the declining V1–V2–PPC–PFC gradient in the GABA composite measures might reflect regional differences in the GABA neuron density, which is greater in V1 than in PFC (Hendry et al. 1987; Kritzer et al. 1992; Kritzer and Goldman-Rakic 1995; DeFelipe et al. 1999; Kondo et al. 1999; Collins et al. 2016).

Consistent with our prediction that glutamate and GABA transcripts in layer 3 would both reach mature levels prior to the adult period, we found that adult-like gradients for glutamate transcripts emerged during the prepubertal period (3–19 months of age), whereas those for GABA transcripts emerged later during the peripubertal period (30–47 months of age). The earlier emergence of glutamate than GABA adult-like gradients has been observed for other functional measures in layer 3 of monkey PFC. For example, multiple refinements to glutamatergic synapses occur during the prepubertal period, including changes in the relative contributions of glutamatergic AMPA and NMDA receptor properties (Gonzalez-Burgos et al. 2008) that can support adult-like levels of activity. The appearance of the adult pattern of increasing V1–V2–PPC–PFC glutamate composite levels during the prepubertal period was driven primarily by increasing glutamate composite levels in the PFC without developmental changes in V1. These findings are supported by studies which found that multiple pyramidal neuron properties, including synapse profiles, had more protracted developmental changes in PFC than in V1 (Guillery 2005; Elston and Fujita 2014). In contrast, some molecular markers of GABA synapses (e.g., parvalbumin immunoreactivity in the axon terminals of basket and chandelier GABA neurons) exhibit protracted postnatal changes through the peripubertal period in layer 3 of monkey PFC (Anderson et al. 1995; Fish et al. 2013). In addition, RNA sequencing data from human postmortem PFC, although they lack laminar specificity, have reported similar regional patterns for the glutamate and GABA transcripts studied here (Jaffe et al. 2018). Thus, the temporal differences in the emergence of adult-like gradients for glutamate and GABA composite measures might index key functional refinements in layer 3 pyramidal and interneuron microcircuits.

Finally, we predicted that developmental trajectories for glutamate and GABA measures would be more protracted in layer 3 than in layer 6, given prior findings supporting an “inside-out” laminar pattern of cortical development (Rakic 1974; Bystron et al. 2008). However, this prediction turned out to not be testable as formulated because layer 6 did not exhibit V1–V2–PPC–PFC gradients in glutamate or GABA markers for any age group. The marked differences between layers 3 and 6 in their patterns of glutamate transcript gradients across the monkey vsWM network may reflect, at least in part, differences between these layers in developmental changes in dendritic spine density (Bourgeois and Rakic 1993; Bourgeois et al. 1994; Oga et al. 2017). For example, in human and monkey PFC, overproduction and pruning of dendritic spines and axospinous synapses are more pronounced in layer 3 than in deeper layers (Bourgeois et al. 1994; Huttenlocher and Dabholkar 1997; Petanjek et al. 2011). In addition, layer 3 pyramidal neurons have more protracted developmental increases in soma size, dendritic arbor growth, and dendritic complexity relative to deeper layer pyramidal neurons (Petanjek et al. 2008). Similarly, the laminar differences in GABA transcripts might be related to prior findings that the maturation of GABA neurons occurs much earlier in the deep than in the superficial cortical layers (Condé et al. 1996; Miyoshi and Fishell 2011; Zecevic et al. 2011). It is also important to note that this current study involved between-subject, cross-sectional measures and thus cannot be interpreted as within-subject, longitudinal developmental data.

Implications for vsWM Function

The regional differences in the glutamate composite measure in layer 3 reported here are supported by findings in macaque neocortex that the number of dendritic spines, the principal site of excitatory synapses, on layer 3 pyramidal neurons is ~10 times higher in the PFC than in V1 (Elston 2000; Elston et al. 2001; Chaudhuri et al. 2015; Medalla and Luebke 2015). In addition, since roughly 80% of the excitatory inputs in the neocortex are from local sources (McGuire et al. 1991; Markov et al. 2014), this regional difference in the dendritic spine number is consistent with findings that the number of recurrent excitatory connections, an important substrate for delay period activity during vsWM (Goldman-Rakic 1995; Wang 2001), is greater for layer 3 pyramidal neurons in the PFC than in V1 (Levitt et al. 1993; Lund et al. 1993; Kritzer and Goldman-Rakic 1995; Pucak et al. 1996). Lateral connectivity, which is also thought to be an anatomical substrate for recurrent excitation, has a gradient that also increases from primary to higher-order association cortex (Goldman-Rakic 1996; Elston 2000) similar to the dendritic spine density. These patterns have been proposed to endow neurons in association cortices with longer intrinsic temporal stability and integrative capacity (Jacobs and Scheibel 2002; Elston 2003; Spruston 2008; Murray et al. 2014; Luebke 2017; Wasmuht et al. 2018), perhaps enhancing the capacity of such neurons to carry information during vsWM tasks (Wasmuht et al. 2018). Importantly, preclinical studies have shown that the expression level of vGLUT1 determines the amount of glutamate that is filled into vesicles and released to regulate excitatory neurotransmission (Bellocchio 2000; Takamori et al. 2000; Du et al. 2020), and both preclinical and clinical studies have linked changes in glutamate neurotransmission to cognitive impairment (Kugaya and Sanacora 2005; Robbins and Murphy 2006). Therefore, higher levels of vGLUT1 mRNA in the PFC might index a greater density of presynaptic glutamate terminals and an increased functional capacity for glutamate neurotransmission required for optimal vsWM function.

The GABA composite measure in layer 3 across the vsWM network may reflect regional differences in the GABA neuron number and subtypes. For example, the density of GABA neurons is higher in V1 than in the PFC (Hendry et al. 1987; Kritzer et al. 1992; Kritzer and Goldman-Rakic 1995; DeFelipe et al. 1999; Kondo et al. 1999; Collins et al. 2016). Recent studies in rodents, monkeys, and humans also suggest that the ratio of somatostatin-containing to parvalbumin-containing GABA neurons increases from the primary sensory to higher-order association cortices (Liu et al. 2012; Kim et al. 2017; Tsubomoto et al. 2019; Anderson et al. 2020). These findings are consistent with a "dendritic disinhibition, pathway gating" hypothesis which posits that cortical areas needing to integrate converging inputs from many different pathways (such as the PFC when engaged in vsWM) require a higher contribution of GABA neurons that target dendrites (i.e., somatostatin-containing GABA neurons) (Wang and Yang 2018).

It is important to note that the glutamate and GABA composite measures used in the present study capture a limited number of gene products that regulate glutamate or GABA neurotransmission, constraining interpretations for vsWM function of the observed regional gradients. In addition, although gene transcription can serve as a proxy for protein levels and subsequently function, interpreting mRNA findings requires caution and further study at the cognate protein and physiological levels. For example, additional informative patterns might be reflected at the level of epigenetic modifications, protein expression, mRNA and protein degradation/turnover, or neuronal activity rather than at the level of transcript expression. Finally, using RNA sequencing techniques would be an excellent way to better understand global transcriptomic profiles across regions, layers, and development and thus would inform the interpretation and assess potential contributory mechanisms for these findings (Zhu et al. 2018).

Finally, since all but one of the subjects in this study were female, we are unable to directly examine the potential sex differences in the expression patterns of these glutamate and GABA transcripts. However, recent human databases allow for examination of potential sex differences in the typical adult human brain, at least in the PFC. Examination of the available information in the Genotype-Tissue Expression Project (GTEx) and BrainSpan databases did not reveal prominent sex differences for the transcripts analyzed in this study (Kang et al. 2011, BrainSpan Portal accessed on 17 August 2020; The GTEx Consortium 2013, GTEx Portal accessed on 17 August 2020). However, the available information cannot exclude possible sex differences for a given transcript in other cortical regions, in a specific cortical layer, or at a certain developmental age.

Implications for Altered Glutamate and GABA Neurotransmission in the vsWM Network in Schizophrenia

In this study, we found that the glutamate composite measure achieved the adult-like gradient earlier in development than the GABA composite measure. The appearance of the adult-like glutamate gradient appeared to be driven principally by an increase of the glutamate composite measure in the PFC, whereas the appearance of the adult-like gradient for the GABA measure appeared to be driven principally by an increase of the GABA composite measure in V1. These findings suggest that among the developmental risk factors for schizophrenia (Lewis and Levitt 2002; van Os et al. 2010), those affecting glutamate neurotransmission might be more likely to impact PFC neural circuits, whereas those affecting GABA neurotransmission might be more likely to impact V1 neural circuits. In our prior study of the vsWM cortical network in schizophrenia, we found that the glutamate and GABA composite measures in layer 3 were both lower in the PFC and higher in V1 relative to comparison subjects (Hoftman et al. 2018). Together, these findings suggest the speculative interpretation that schizophrenia is associated with a blunted developmental increase in glutamate transmission in the PFC, which evokes a compensatory downregulation of GABA neurotransmission, whereas an excessive developmental increase in GABA neurotransmission in V1 evokes a compensatory upregulation of glutamate neurotransmission in V1. Further studies in schizophrenia of additional measures of glutamate and GABA neurotransmission in layer 3 of both V1 and PFC are needed to test this interpretation, but this scenario could explain why glutamatergic or GABAergic agents that act broadly across the vsWM network have failed to show replicated positive effects on the vsWM function in schizophrenia.

The presence of glutamate and GABA composite measure gradients in layer 3, but not in layer 6, might also contribute to the apparent preferential vulnerability of layer 3 circuitry to the alterations in schizophrenia. For example, postmortem studies of schizophrenia have consistently reported lower dendritic spine densities and smaller pyramidal neuron soma volumes in layer 3 across cortical regions (Garey et al. 1998; Rajkowska et al. 1998; Selemon et al. 1998; Glantz and Lewis 2000; Sweet

et al. 2003; Dorph-Petersen et al. 2007; Glausier and Lewis 2013; Konopaske et al. 2014), whereas such alterations were not detected in layer 6 (Rajkowska et al. 1998; Kolluri et al. 2005). Similarly, measures of GAD67 mRNA were altered in layer 3 but not in layer 6 (Akbarian et al. 1995; Volk et al. 2000).

Together, these findings suggest that the alterations in vsWM function in schizophrenia might arise due to region- and layer-specific disturbances in the development of cortical glutamate and GABA neurotransmission.

Supplementary Material

Supplementary material can be found at *Cerebral Cortex* online.

Notes

Special thanks to Mary Brady and Kelly Rogers for their technical expertise. *Conflict of Interest*: David A. Lewis currently receives investigator-initiated research support from Pfizer and Merck, and serves as a paid consultant on basic science research for Astellas.

Funding

National Institute of Health (grant MH051234) and NIMH MD/PhD R01 Supplement.

References

Akbarian S, Kim JJ, Potkin SG, Hagman JO, Tafazzoli A, Bunney WE Jr, Jones EG. 1995. Gene expression for glutamic acid decarboxylase is reduced without loss of neurons in prefrontal cortex of schizophrenics. *Arch Gen Psychiatry*. 52:258–266.

Anderson KM, Collins MA, Chin R, Ge T, Rosenberg MD, Holmes AJ. 2020. The transcriptional landscape of cortical interneurons underlies in-vivo brain function and schizophrenia risk. *Nat Commun*. 11:2889–2904.

Anderson SA, Classey JD, Condé F, Lund JS, Lewis DA. 1995. Synchronous development of pyramidal neuron dendritic spines and parvalbumin-immunoreactive chandelier neuron axon terminals in layer III of monkey prefrontal cortex. *Neuroscience*. 67:7–22.

Arnsten AF. 2015. Stress weakens prefrontal networks: molecular insults to higher cognition. *Nat Neurosci*. 18:1376–1385.

Baddeley A. 1992. Working memory. *Science*. 255:556–559.

Barch DM, Ceaser A. 2012. Cognition in schizophrenia: core psychological and neural mechanisms. *Trends Cogn Sci*. 16:27–34.

Bellocchio EE. 2000. Uptake of glutamate into synaptic vesicles by an inorganic phosphate transporter. *Science*. 289:957–960.

Bourgeois JP, Goldman-Rakic PS, Rakic P. 1994. Synaptogenesis in the prefrontal cortex of rhesus monkeys. *Cereb Cortex*. 4:78–96.

Bourgeois JP, Rakic P. 1993. Changes of synaptic density in the primary visual cortex of the macaque monkey from fetal to adult stage. *J Neurosci*. 13:2801–2820.

Bystron I, Blakemore C, Rakic P. 2008. Development of the human cerebral cortex: Boulder Committee revisited. *Nat Rev Neurosci*. 9:110–122.

Chaudhuri R, Knoblauch K, Gariel MA, Kennedy H, Wang XJ. 2015. A large-scale circuit mechanism for hierarchical dynamical processing in the primate cortex. *Neuron*. 88:419–431.

Chung DW, Wills ZP, Fish KN, Lewis DA. 2017. Developmental pruning of excitatory synaptic inputs to parvalbumin interneurons in monkey prefrontal cortex. *Proc Natl Acad Sci U S A*. 114:E629–E637.

Collins CE, Turner EC, Sawyer EK, Reed JL, Young NA, Flaherty DK, Kaas JH. 2016. Cortical cell and neuron density estimates in one chimpanzee hemisphere. *Proc Natl Acad Sci U S A*. 113:740–745.

Condé F, Lund JS, Jacobowitz DM, Baimbridge KG, Lewis DA. 1994. Local circuit neurons immunoreactive for calretinin, calbindin D-28k, or parvalbumin in monkey prefrontal cortex: distribution and morphology. *J Comp Neurol*. 341:95–116.

Condé F, Lund JS, Lewis DA. 1996. The hierarchical development of monkey visual cortical regions as revealed by the maturation of parvalbumin-immunoreactive neurons. *Dev Brain Res*. 96:261–276.

Datta D, Arion D, Lewis DA. 2015. Developmental expression patterns of GABAA receptor subunits in layer 3 and 5 pyramidal cells of monkey prefrontal cortex. *Cereb Cortex*. 25:2295–2305.

DeFelipe J, Del Río MR, González-Albo MC, Elston GN. 1999. Distribution and patterns of connectivity of interneurons containing calbindin, calretinin and parvalbumin in visual areas of the occipital and temporal lobes of the macaque monkey. *J Comp Neurol*. 412:515–526.

Dienel SJ, Bazmi HH, Lewis DA. 2017. Development of transcripts regulating dendritic spines in layer 3 pyramidal cells of the monkey prefrontal cortex: implications for the pathogenesis of schizophrenia. *Neurobiol Dis*. 105:132–141.

Dienel SJ, Enwright JF 3rd, Hoftman GD, Lewis DA. 2019. Markers of glutamate and GABA neurotransmission in the prefrontal cortex of schizophrenia subjects: disease effects differ across anatomical levels of resolution. *Schizophr Res*. 217:86–94.

Dorph-Petersen KA, Pierri JN, Wu Q, Sampson AR, Lewis DA. 2007. Primary visual cortex volume and total neuron number are reduced in schizophrenia. *J Comp Neurol*. 501:290–301.

Du X, Li J, Li M, Yang X, Qi Z, Xu B, Lui W, Xu Z, Deng Y. 2020. Research progress on the role of type I vesicular glutamate transporter (VGLUT1) in nervous system diseases. *Cell Biosci*. 10:26–36.

Elston GN. 2000. Pyramidal cells of the frontal lobe: all the more spinous to think with. *J Neurosci*. 20:RC95.

Elston GN, Benavides-Piccione R, De Felipe J. 2001. The pyramidal cell in cognition: a comparative study in human and monkey. *J Neurosci*. 21:RC163–RC167.

Elston GN. 2003. Cortex, cognition and the cell: new insights into the pyramidal neuron and prefrontal function. *Cereb Cortex*. 13:1124–1138.

Elston GN, Fujita I. 2014. Pyramidal cell development: postnatal spinogenesis, dendritic growth, axon growth, and electrophysiology. *Front Neuroanat*. 8:78. doi: 10.3389/fnana.2014.00078pmid:25161611.

Felleman DJ, Van Essen DC. 1991. Distributed hierarchical processing in the primate cerebral cortex. *Cereb Cortex*. 1:1–47.

Fish KN, Hoftman GD, Sheikh W, Kitchens M, Lewis DA. 2013. Parvalbumin-containing chandelier and basket cell boutons have distinctive modes of maturation in monkey prefrontal cortex. *J Neurosci*. 33:8352–8358.

Garey LJ, Ong WY, Patel TS, Kanani M, Davis A, Mortimer AM, Barnes TR, Hirsch SR. 1998. Reduced dendritic spine density

on cerebral cortical pyramidal neurons in schizophrenia. *J Neurol Neurosurg Psychiatry*. 65:446–453.
Glantz LA, Lewis DA. 2000. Decreased dendritic spine density on prefrontal cortical pyramidal neurons in schizophrenia. *Arch Gen Psychiatry*. 57:65–73.
Glausier JR, Lewis DA. 2013. Dendritic spine pathology in schizophrenia. *Neuroscience*. 251:90–107.
Goldman-Rakic PS. 1995. Cellular basis of working memory. *Neuron*. 14:477–485.
Goldman-Rakic PS. 1996. Regional and cellular fractionation of working memory. *Proc Natl Acad Sci U S A*. 93:13473–13480.
Gonzalez-Burgos G, Kroener S, Zaitsev AV, Povysheva NV, Krimer LS, Barrionuevo G, Lewis DA. 2008. Functional maturation of excitatory synapses in layer 3 pyramidal neurons during postnatal development of the primate prefrontal cortex. *Cereb Cortex*. 18:626–637.
Gonzalez-Burgos G, Miyamae T, Krimer Y, Gulchina Y, Pafundo DE, Krimer O, Bazmi H, Arion D, Enwright JF, Fish KN, et al. 2019. Distinct properties of layer 3 pyramidal neurons from prefrontal and parietal areas of the monkey neocortex. *J Neurosci*. 39:7277–7290.
Guillery RW. 2005. Is postnatal neocortical maturation hierarchical? *Trends Neurosci*. 28:512–517.
Hawrylycz MJ, Lein ES, Guillozet-Bongaarts AL, Shen EH, Ng L, Miller JA, van de Lagemaat LN, Smith KA, Ebbert A, Riley ZL, et al. 2012. An anatomically comprehensive atlas of the adult human brain transcriptome. *Nature*. 489:391–399.
Hendry SH, Schwark HD, Jones EG, Yan J. 1987. Numbers and proportions of GABA-immunoreactive neurons in different areas of monkey cerebral cortex. *J Neurosci*. 7:1503–1519.
Hoftman GD, Dienel SJ, Bazmi HH, Zhang Y, Chen K, Lewis DA. 2018. Altered gradients of glutamate and gamma-aminobutyric acid transcripts in the cortical visuospatial working memory network in schizophrenia. *Biol Psychiatry*. 83:670–679.
Hoftman GD, Volk DW, Bazmi HH, Li S, Sampson AR, Lewis DA. 2015. Altered cortical expression of GABA-related genes in schizophrenia: illness progression vs developmental disturbance. *Schizophr Bull*. 41:180–191.
Huttenlocher PR, Dabholkar AS. 1997. Regional differences in synaptogenesis in human cerebral cortex. *J Comp Neurol*. 387:167–178.
Jacobs B, Scheibel AB. 2002. Regional dendritic variation in primate cortical pyramidal cells. In: Schüz A, Miller R, editors. *Cortical areas: unity and diversity*. London: Taylor and Francis, pp. 111–131.
Jaffe AE, Straub RE, Shin JH, Tao R, Gao Y, Collado-Torres L, Kam-Thong T, Xi HS, Quan J, Chen Q, et al. 2018. Developmental and genetic regulation of the human cortex transcriptome illuminate schizophrenia pathogenesis. *Nat Neurosci*. 21:1117–1125.
Jones EG. 1984. Laminar distribution of cortical efferent cells. In: Peters A, Jones EG, editors. *Cerebral cortex*. Vol 1. New York, NY: Plenum Press, pp. 521–553.
Kang HJ, Kawasawa YI, Cheng F, Zhu Y, Xu X, Li M, Sousa AM, Pletikos M, Meyer KA, Sedmak G, et al. 2011. Spatio-temporal transcriptome of the human brain. *Nature*. 478:483–489.
Kim Y, Yang GR, Pradhan K, Venkataraju KU, Bota M, Del Molino LCG, Fitzgerald G, Ram K, He M, Levine JM, et al. 2017. Brain-wide maps reveal stereotyped cell-type-based cortical architecture and subcortical sexual dimorphism. *Cell*. 171: 456–469.e22.
Kolluri N, Sun Z, Sampson AR, Lewis DA. 2005. Lamina-specific reductions in dendritic spine density in the prefrontal cortex of subjects with schizophrenia. *Am J Psychiatry*. 162:1200–1202.
Kondo HT, Tanaka K, Hashikawa T, Jones EG. 1999. Neurochemical gradients along monkey sensory cortical pathways: calbindin-immunoreactive pyramidal neurons in layers II and III. *Eur J Neurosci*. 11:4197–4203.
Konopaske GT, Lange N, Coyle JT, Benes FM. 2014. Prefrontal cortical dendritic spine pathology in schizophrenia and bipolar disorder. *JAMA Psychiat*. 71:1323–1331.
Kritzer MF, Cowey A, Somogyi P. 1992. Patterns of inter- and intralaminar GABAergic connections distinguish striate (V1) and extrastriate (V2, V4) visual cortices and their functionally specialized subdivisions in the rhesus monkeys. *J Neurosci*. 12:4545–4564.
Kritzer MF, Goldman-Rakic PS. 1995. Intrinsic circuit organization of the major layers and sublayers of the dorsolateral prefrontal cortex in the rhesus monkey. *J Comp Neurol*. 359:131–143.
Kugaya A, Sanacora G. 2005. Beyond monoamines: glutamatergic function in mood disorders. *CNS Spectr*. 10:808–819.
Lardi-Studler B, Fritschy JM. 2007. Matching of pre- and postsynaptic specializations during synaptogenesis. *Neuroscientist*. 13:115–126.
Levitt JB, Lewis DA, Yoshioka T, Lund JS. 1993. Topography of pyramidal neuron intrinsic connections in macaque monkey prefrontal cortex (areas 9 and 46). *J Comp Neurol*. 338:360–376.
Lewis DA, Levitt P. 2002. Schizophrenia as a disorder of neurodevelopment. *Annu Rev Neurosci*. 25:409–432.
Lewis JW, Van Essen DC. 2000. Mapping of architectonic subdivisions in the macaque monkey, with emphasis on parieto-occipital cortex. *J Comp Neurol*. 428:79–111.
Linden DE. 2007. The working memory networks of the human brain. *Neuroscientist*. 13:257–267.
Liu X, Somel M, Tang L, Yan Z, Jiang X, Guo S, Yuan Y, He L, Oleksiak A, Zhang Y, et al. 2012. Extension of cortical synaptic development distinguishes humans from chimpanzees and macaques. *Genome Res*. 22:611–622.
Luebke JI. 2017. Pyramidal neurons are not generalizable building blocks of cortical networks. *Front Neuroanat*. doi: 10.3389/fnana.2017.00011.
Lund JS, Boothe RG, Lund RD. 1977. Development of neurons in the visual cortex (area 17) of the monkey (*Macaca nemestrina*): a Golgi study from fetal day 127 to postnatal maturity. *J Comp Neurol*. 176:149–187.
Lund JS, Yoshioka T, Levitt JB. 1993. Comparison of intrinsic connectivity in different areas of macaque monkey cerebral cortex. *Cereb Cortex*. 3:148–162.
Markov NT, Ercsey-Ravasz MM, Ribeiro Gomes AR, Lamy C, Magrou L, Vezoli J, Misery P, Falchier A, Quilodran R, Gariel MA, et al. 2014. A weighted and directed interareal connectivity matrix for macaque cerebral cortex. *Cereb Cortex*. 24: 17–36.
McGuire BA, Gilbert CD, Rivlin PK, Wiesel TN. 1991. Targets of horizontal connections in macaque primary visual cortex. *J Comp Neurol*. 305:370–392.
Medalla M, Luebke JI. 2015. Diversity of glutamatergic synaptic strength in lateral prefrontal versus primary visual cortices in the rhesus monkey. *J Neurosci*. 35:112–127.
Miller EK, Cohen JD. 2001. An integrative theory of prefrontal cortex function. *Annu Rev Neurosci*. 24:167–202.

Miyoshi G, Fishell G. 2011. GABAergic interneuron lineages selectively sort into specific cortical layers during early postnatal development. *Cereb Cortex*. 21:845–852.

Murray JD, Bernacchia A, Freedman DJ, Romo R, Wallis JD, Cai X, Padoa-Schioppa C, Pasternak T, Seo H, Lee D, et al. 2014. A hierarchy of intrinsic timescales across primate cortex. *Nat Neurosci*. 17:1661–1663.

Niendam TA, Ray KL, Iosif AM, Lesh TA, Ashby SR, Patel PK, Smucny J, Ferrer E, Solomon M, Ragland JD, et al. 2018. Association of age at onset and longitudinal course of prefrontal function in youth with schizophrenia. *JAMA Psychiat*. 75:1252–1260.

Oga T, Elston GN, Fujita I. 2017. Postnatal dendritic growth and spinogenesis of layer V pyramidal cells differ between visual, inferotemporal, and prefrontal cortex of the macaque monkey. *Front Neuroanat*. 11:118. doi: 10.3389/fnins.2017.00118.

Pandya DN, Seltzer B. 1982. Intrinsic connections and architectonics of posterior parietal cortex in the rhesus monkey. *J Comp Neurol*. 204:196–210.

Petanjek Z, Judas M, Kostovic I, Uylings HB. 2008. Lifespan alterations of basal dendritic trees of pyramidal neurons in the human prefrontal cortex: a layer-specific pattern. *Cereb Cortex*. 18:915–929.

Petanjek Z, Judas M, Simic G, Rasin MR, Uylings HB, Rakic P, Kostovic I. 2011. Extraordinary neoteny of synaptic spines in the human prefrontal cortex. *Proc Natl Acad Sci U S A*. 108:13281–13286.

Pucak ML, Levitt JB, Lund JS, Lewis DA. 1996. Patterns of intrinsic and associational circuitry in monkey prefrontal cortex. *J Comp Neurol*. 376:614–630.

Rajkowska G, Selemon LD, Goldman-Rakic PS. 1998. Neuronal and glial somal size in the prefrontal cortex: a postmortem morphometric study of schizophrenia and Huntington disease. *Arch Gen Psychiatry*. 55:215–224.

Rakic P. 1974. Neurons in rhesus monkey visual cortex: systematic relation between time of origin and eventual disposition. *Science*. 183:425–427.

Rakic P. 2009. Evolution of the neocortex: a perspective from developmental biology. *Nat Rev Neurosci*. 10:724–735.

Rakic P, Bourgeois JP, Eckenhoff MF, Zecevic N, Goldman-Rakic PS. 1986. Concurrent overproduction of synapses in diverse regions of the primate cerebral cortex. *Science*. 232: 232–235.

Reichenberg A, Caspi A, Harrington H, Houts R, Keefe RS, Murray RM, Poulton R, Moffitt TE. 2010. Static and dynamic cognitive deficits in childhood preceding adult schizophrenia: a 30-year study. *Am J Psychiatry*. 167:160–169.

Robbins TW, Murphy ER. 2006. Behavioral pharmacology: 40+ years of progress, with a focus on glutamate receptors and cognition. *Trends Pharmacol Sci*. 27:141–148.

Rockland KS. 1997. Elements Of cortical architecture: hierarchy revisited. In: Rockland K, Kaas JH, Peters A, editors. *Cerebral cortex vol 12, extrastriate cortex in primates*. New York: Plenum, pp. 243–293.

Selemon LD, Rajkowska G, Goldman-Rakic PS. 1998. Elevated neuronal density in prefrontal area 46 in brains from schizophrenic patients: application of a three-dimensional, stereologic counting method. *J Comp Neurol*. 392:402–412.

Sowell ER, Peterson BS, Thompson PM, Welcome SE, Henkenius AL, Toga AW. 2003. Mapping cortical change across the human life span. *Nat Neurosci*. 6:309–315.

Spruston N. 2008. Pyramidal neurons: dendritic structure and synaptic integration. *Nat Rev Neurosci*. 9:206–221.

Sweet RA, Pierri JN, Auh S, Sampson AR, Lewis DA. 2003. Reduced pyramidal cell somal volume in auditory association cortex of subjects with schizophrenia. *Neuropsychopharmacology*. 28:599–609.

Takamori S, Rhee JS, Rosenmund C, Jahn R. 2000. Identification of a vesicular glutamate transporter that defines a glutamatergic phenotype in neurons. *Nature*. 407:189–194.

Tamnes CK, Ostby Y, Fjell AM, Westlye LT, Due-Tonnessen P, Walhovd KB. 2010. Brain maturation in adolescence and young adulthood: regional age-related changes in cortical thickness and white matter volume and microstructure. *Cereb Cortex*. 20:534–548.

The GTEx Consortium. 2013. The genotype-tissue expression (GTEx) project. *Nat Genet*. 45:580–585.

Tsubomoto M, Kawabata R, Zhu X, Minabe Y, Chen K, Lewis DA, Hashimoto T. 2019. Expression of transcripts selective for GABA neuron subpopulations across the cortical visuospatial working memory network in the healthy state and schizophrenia. *Cereb Cortex*. 29:3540–3550.

van Os J, Kenis G, Rutten BP. 2010. The environment and schizophrenia. *Nature*. 468:203–212.

Volk DW, Austin MC, Pierri JN, Sampson AR, Lewis DA. 2000. Decreased glutamic acid decarboxylase67 messenger RNA expression in a subset of prefrontal cortical gamma-aminobutyric acid neurons in subjects with schizophrenia. *Arch Gen Psychiatry*. 57:237–245.

Walker AE. 1940. A cytoarchitectural study of the prefrontal area of the macaque monkey. *J Comp Neurol*. 73:59–86.

Wang XJ. 2001. Synaptic reverberation underlying mnemonic persistent activity. *Trends Neurosci*. 24:455–463.

Wang XJ, Tegner J, Constantinidis C, Goldman-Rakic PS. 2004. Division of labor among distinct subtypes of inhibitory neurons in a cortical microcircuit of working memory. *Proc Natl Acad Sci U S A*. 101:1368–1373.

Wang XJ, Yang GR. 2018. A disinhibitory circuit motif and flexible information routing in the brain. *Curr Opin Neurobiol*. 49:75–83.

Wasmuht DF, Spaak E, Buschman TJ, Miller EK, Stokes MG. 2018. Intrinsic neuronal dynamics predict distinct functional roles during working memory. *Nat Commun*. 9:3499.

Zecevic N, Hu F, Jakovcevski I. 2011. Interneurons in the developing human neocortex. *Dev Neurobiol*. 71:18–33.

Zhu Y, Sousa AMM, Gao T, Skarica M, Li M, Santpere G, Esteller-Cucala P, Juan D, Ferrandez-Peral L, Gulden FO, et al. 2018. Spatiotemporal transcriptomic divergence across human and macaque brain development. *Science*. 362:6420–6435.